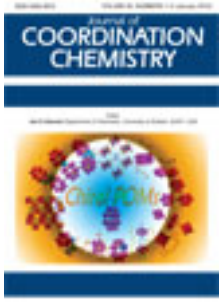

Journal of Coordination Chemistry
Publication details, including instructions for authors and subscription information:
http://www.tandfonline.com/loi/gcoo20

Synthesis, DNA-binding, photocleavage, cytotoxicity, and apoptosis studies of ruthenium(II) complexes containing 3,6-dimethyldipyrido[3,2-a:2′,3′-c]phenazine

Li Xu [a], Nan-Jing Zhong [b], Yang-Yin Xie [c], Hong-Liang Huang [d], Zhen-Hua Liang [c], Zheng-Zheng Li [c] & Yun-Jun Liu [c]

[a] School of Chemistry and Chemical Engineering, Guangdong Pharmaceutical University, Zhongshan 528458, PR China

[b] School of Food Science, Guangdong Pharmaceutical University, Zhongshan 528458, PR China

[c] School of Pharmacy, Guangdong Pharmaceutical University, Guangzhou 510006, PR China

[d] School of Life Science and Biopharmacology, Guangdong Pharmaceutical University, Guangzhou 510006, PR China

Published online: 14 Dec 2011.

To cite this article: Li Xu, Nan-Jing Zhong, Yang-Yin Xie, Hong-Liang Huang, Zhen-Hua Liang, Zheng-Zheng Li & Yun-Jun Liu (2012) Synthesis, DNA-binding, photocleavage, cytotoxicity, and apoptosis studies of ruthenium(II) complexes containing 3,6-dimethyldipyrido[3,2-a:2′,3′-c]phenazine, Journal of Coordination Chemistry, 65:1, 55-68, DOI: 10.1080/00958972.2011.640675

To link to this article: http://dx.doi.org/10.1080/00958972.2011.640675

Journal of Coordination Chemistry
Vol. 65, No. 1, 10 January 2012, 55–68

Synthesis, DNA-binding, photocleavage, cytotoxicity, and apoptosis studies of ruthenium(II) complexes containing 3,6-dimethyldipyrido[3,2-a:2′,3′-c]phenazine

LI XU†, NAN-JING ZHONG‡, YANG-YIN XIE§, HONG-LIANG HUANG*¶, ZHEN-HUA LIANG§, ZHENG-ZHENG LI§ and YUN-JUN LIU*§

†School of Chemistry and Chemical Engineering, Guangdong Pharmaceutical University, Zhongshan 528458, PR China
‡School of Food Science, Guangdong Pharmaceutical University, Zhongshan 528458, PR China
§School of Pharmacy, Guangdong Pharmaceutical University, Guangzhou 510006, PR China
¶School of Life Science and Biopharmacology, Guangdong Pharmaceutical University, Guangzhou 510006, PR China

(*Received 5 October 2011; in final form 2 November 2011*)

Two new ruthenium(II) polypyridyl complexes, $[Ru(bpy)_2(DMDPPZ)](ClO_4)_2$ (**1**) (bpy = 2,2′-bipyridine, DMDPPZ = 3,6-dimethyldipyrido[3,2-a:2′,3′-c]phenazine) and $[Ru(dmb)_2(DMDPPZ)](ClO_4)_2$ (**2**) (dmb = 4,4′-dimethyl-2,2′-bipyridine), have been synthesized and their DNA-binding, photoinduced DNA cleavage, and cell cytotoxicity are studied. The complexes show good binding to calf thymus DNA in the order: **1** > **2**. Both complexes exhibit efficient DNA cleavage upon irradiation *via* a mechanistic pathway involving formation of singlet oxygen as the reactive species. The cytotoxic activity of **1** and **2** was tested by the 3-(4,5-dimethylthiazol-2-yl)-2,5-diphenyl-2*H*-tetrazolium bromide (MTT) method. These complexes effectively inhibit the proliferation of tumor cells. The antioxidant activity against hydroxyl radical (•OH) was also explored.

Keywords: Ruthenium complexes; Cytotoxicity; DNA-binding; Apoptosis; Antioxidant activity

1. Introduction

Clinical use of *cis*-diamminedichloroplatinum(II) (cisplatin) and other metal complexes in treatment of human cancer has stimulated studies of interactions of nucleic acids (DNA) with different metal complexes due to their potential applications as chemical and stereoselective probes of nucleic acid structures, as molecular ''light switches'', and as anticancer drugs or complexes with other biological functions [1–5]. Ruthenium(II) polypyridine complexes, due to a combination of easily constructed rigid chiral structures spanning all three spatial dimensions and a rich photophysical repertoire, are

*Corresponding authors. Email: honglianghuangcn@hotmail.com; lyjche@163.com

ISSN 0095-8972 print/ISSN 1029-0389 online © 2012 Taylor & Francis
http://dx.doi.org/10.1080/00958972.2011.640675

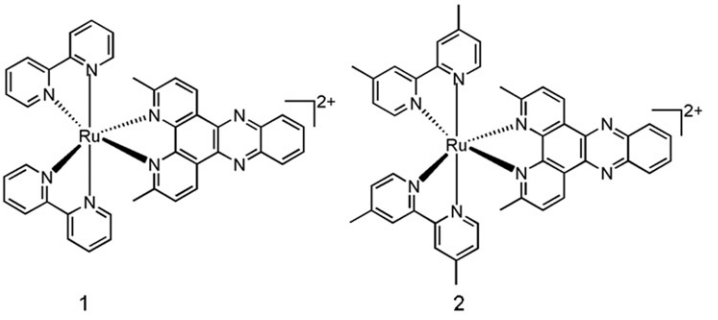

Scheme 1. The structures of **1** and **2**.

regarded as promising candidates and several ruthenium complexes have now been proposed as potential anticancer substances, demonstrating remarkable anticancer activity and showing lower general toxicity [6–10]. Among these complexes, the Ru(II)-dppz complexes with bidentate ancillary ligands (co-ligands), e.g., bpy, phen, dmb, dmp, etc., have been reported for their interesting properties [11–13]. Changing substituent groups in the intercalative ligand can also create differences in the space configuration and electron density distribution of Ru(II) polypyridine complexes, resulting in different spectral properties, DNA-binding behaviors, photocleavage properties, and even their biological activities *in vitro*. In this article, we report the synthesis and characterization of two new ruthenium(II) polypyridine complexes, $[Ru(bpy)_2(DMDPPZ)](ClO_4)_2$ (**1**) (bpy = 2,2′-bipyridine, DMDPPZ = 3,6-dimethyldipyrido[3,2-a:2′,3′-c]phenazine) and $[Ru(dmb)_2(DMDPPZ)](ClO_4)_2$ (**2**) (dmb = 4,4′-dimethyl-2,2′-bipyridine, scheme 1). Their DNA-binding behaviors were studied by electronic absorption titration, viscosity measurements, and photoactivated cleavage. The results indicate that **1** and **2** intercalate between base pairs of DNA. The cytotoxicities of **1** and **2** have been evaluated by MTT assay, showing that these complexes exhibit high activity against MCF-7 (breast cancer), Hela (epithelial carcinoma), BEL-7402 (hepatocellular carcinoma), and MG-63 (osteosarcoma) cells in a dose-dependent manner. The results obtained from the apoptosis assay show that these complexes can induce apoptosis of BEL-7402 cells and experiments on antioxidant activity of these complexes against hydroxyl radical (•OH) were also explored.

2. Experimental

2.1. *Materials and methods*

Calf thymus DNA (CT-DNA) was obtained from the Sino-American Biotechnology Company. pBR 322 DNA was obtained from Shanghai Sangon Biological Engineering & Services Co., Ltd. Dimethyl sulfoxide (DMSO) and RPMI 1640 were purchased from Sigma. Cell lines of MCF-7, Hela, BEL-7402, and MG-63 were purchased from American Type Culture Collection; agarose and ethidium bromide (EB) were obtained

from Aldrich. $RuCl_3 \cdot xH_2O$ was purchased from Kunming Institution of Precious Metals. 1,10-Phenanthroline was obtained from Guangzhou Chemical Reagent Factory. Doubly distilled water was used to prepare buffers (5 mmol L^{-1} Tris(hydroxymethylaminomethane)-HCl, 50 mmol L^{-1} NaCl, pH = 7.2). A solution of CT-DNA in the buffer gave a ratio of UV absorbance at 260 and 280 nm of *ca* 1.8–1.9 : 1, indicating that DNA was sufficiently free of protein [14]. The DNA concentration per nucleotide was determined by absorption spectroscopy using the molar absorption coefficient (6600 $(mol\,L^{-1})^{-1}\,cm^{-1}$) at 260 nm [15].

Microanalysis (C, H, and N) was carried out with a Perkin-Elmer 240Q elemental analyzer. Electrospray mass spectra (ES-MS) were recorded on a LCQ system (Finnigan MAT, USA) using methanol as the mobile phase. The spray voltage, tube lens offset, capillary voltage, and capillary temperature were set at 4.50 kV, 30.00 V, 23.00 V and 200°C, respectively; the quoted m/z values are for the major peaks in the isotope distribution. ^{1}H NMR spectra were recorded on a Varian-500 spectrometer. All chemical shifts were given relative to tetramethylsilane (TMS). UV-Vis spectra were recorded on a Perkin-Elmer LS 55 spectrofluorophotometer at room temperature.

2.2. *Synthesis and characterization*

Complexes **1** and **2** are mixtures of lambda and delta enantiomers.

2.2.1. Synthesis of $[Ru(bpy)_2(DMDPPZ)](ClO_4)_2$ (1). A mixture of *cis*-$[Ru(bpy)_2Cl_2] \cdot 2H_2O$ (0.288 g, 0.5 mmol) [16] and DMDPPZ [17] (0.155 g, 0.5 mmol) in ethylene glycol (20 cm^3) was refluxed under argon for 8 h to give a clear red solution. Upon cooling, a red precipitate was obtained by dropwise addition of saturated aqueous $NaClO_4$ solution. The crude product was purified by column chromatography on neutral alumina with a mixture of CH_3CN-toluene (3 : 1, v/v) as eluent. The mainly red band was collected, solvent was removed under reduced pressure, and a red powder was obtained. Yield: 70%. Anal. Calcd for $C_{40}H_{30}N_8Cl_2O_8Ru$: C, 52.07; H, 3.28; N, 12.14. Found (%): C, 52.02; H, 3.32; N, 12.10. ES-MS [CH_3CN, m/z]: 822.9 ($[M–ClO_4]^+$), 723.1 ($[M–2ClO_4–H]^+$), 362.3 ($[M–2ClO_4]^{2+}$). ^{1}H NMR (500 MHz, DMSO-d_6): $\delta = 9.63$ (d, 2H, $J = 8.0$ Hz), 8.82 (d, 2H, $J = 8.5$ Hz), 8.77 (d, 2H, $J = 8.0$ Hz), 8.48 (dd, 2 H, $J = 7.8$ Hz), 8.13 (m, 6H), 7.95 (d, 2H, $J = 8.0$ Hz), 7.88 (dd, 2H, $J = 7.7$ Hz), 7.76 (dd, 2H, $J = 7.6$ Hz), 7.41 (dd, 4H, $J = 7.8$ Hz), 2.48 (s, 6H).

2.2.2. Synthesis of $[Ru(dmb)_2(DMDPPZ)](ClO_4)_2$ (2). This complex was synthesized using the same procedure described for **1**. Yield: 68%. Anal. Calcd for $C_{44}H_{38}N_8Cl_2O_8Ru$: C, 53.99; H, 3.91; N, 11.45. Found (%): C, 53.95; H, 3.98; N, 11.41. ES-MS [CH_3CN, m/z]: 879.3 ($[M–ClO_4]^+$), 778.9 ($[M–2ClO_4–H]^+$), 390.1 ($[M–2ClO_4]^{2+}$). ^{1}H NMR (500 MHz, DMSO-d_6): $\delta = 9.59$ (d, 2H, $J = 8.5$ Hz), 8.67 (d, 4H, $J = 8.0$ Hz), 8.48 (d, 2H, $J = 8.2$ Hz), 8.16 (d, 2H, $J = 8.6$ Hz), 7.92 (d, 2H, $J = 8.2$ Hz), 7.68 (d, 2H, $J = 7.6$ Hz), 7.57 (d, 2H, $J = 7.8$ Hz), 7.23 (d, 4H, $J = 8.0$ Hz), 2.49 (s, 6H), 1.92 (s, 12H).

Caution: Perchlorate salts of metal compounds with organic ligands are potentially explosive, and only small amounts of the material should be prepared and handled with great care.

2.3. *DNA-binding and photoactivated cleavage*

The DNA-binding and photoactivated cleavage experiments were performed at room temperature. Buffer A [5 mmol L^{-1} tris(hydroxymethyl)aminomethane (Tris) hydrochloride, 50 mmol L^{-1} NaCl, pH 7.0] was used for absorption titration, luminescence titration, and viscosity measurements. Buffer B (50 mmol L^{-1} Tris-HCl, 18 mmol L^{-1} NaCl, pH 7.2) was used for DNA photocleavage experiments.

The absorption titrations of the complex in buffer were performed using a fixed concentration (10 μmol L^{-1}) for complex to which increments of DNA stock solution were added. Ru-DNA solutions were incubated for 5 min before absorption spectra were recorded. The intrinsic binding constants K, based on the absorption titration, were measured according to the literature [18].

Thermal denaturation studies were carried out with a Perkin-Elmer Lambda 35 spectrophotometer equipped with a Peltier temperature-controlling programmer (±0.1°C). The melting temp (T_m) was taken as the mid-point of the hyperchromic transition. The melting curves were obtained by measuring the absorbance at 260 nm for solutions of CT-DNA (100 μmol L^{-1}) in the absence and presence of Ru^{II} complex (10 μmol L^{-1}) as a function of temperature. The temperature was scanned from 30°C to 95°C at 1°C min^{-1}. The data are presented as $(A - A_0)/(A_f - A_0)$ *versus* T, where A, A_0, and A_f are the observed, the initial, and the final absorbances at 260 nm, respectively.

Viscosity measurements were carried out using an Ubbelodhe viscometer maintained at 25.0 (±0.1)°C in a thermostatic bath. DNA samples approximately 200 base pairs in average length were prepared by sonication to minimize complexities arising from DNA flexibility [19]. The relative viscosity of CT-DNA solution was measured according to the literature [20–22].

For the gel electrophoresis experiment, supercoiled pBR322 DNA (0.1 μg) was treated with the Ru(II) complexes in buffer B, and the solution was then irradiated at room temperature with a UV lamp (365 nm, 10 W). The samples were analyzed by electrophoresis for 1.5 h at 80 V on a 0.8% agarose gel in TBE (89 mmol L^{-1} Tris-borate acid, 2 mmol L^{-1} EDTA, pH = 8.3). The gel was stained with 1 μg mL^{-1} EB and photographed on an Alpha Innotech IS–5500 fluorescence chemiluminescence and visible imaging system.

2.4. *Continuous variation analysis*

Binding stoichiometries were obtained for **1** and **2** with CT-DNA using the method of continuous variation [23]. The concentrations of both complex and DNA were varied, while the sum of the reactant concentrations was kept constant at 50 μmol L^{-1}. The fluorescence intensities of these mixtures were measured at 25°C using an excitation wavelength of 448 and 447 nm. The intensity in fluorescence was plotted *versus* the mole fraction χ of complex to generate a Job's plot.

2.5. *Cell culture and cytotoxicity assay* in vitro

Standard 3-(4,5-dimethylthiazole)-2,5-diphenyltetrazolium bromide (MTT) assay procedures were used [24]. Cells were placed in 96-well microassay culture plates (8×10^3 cells per well) and grown overnight at 37°C in a 5% CO_2 incubator. Compounds tested

were then added to the wells to achieve final concentrations ranging from 10^{-6} to 10^{-4} mol L^{-1}. Control wells were prepared by addition of culture medium (100 μL). The culture medium and cisplatin were used as negative and positive controls, respectively. The plates were incubated at 37°C in a 5% CO_2 incubator for 48 h. Upon completion of the incubation, stock MTT dye solution (20 μL, 5 mg mL^{-1}) was added to each well. After 4 h incubation, buffer (100 μL) containing DMF (50%) and sodium dodecyl sulfate (20%) was added to solubilize the MTT formazan. The optical density of each well was then measured on a microplate spectrophotometer at 490 nm. The IC_{50} values were determined by plotting the percentage viability *versus* concentration on a logarithmic graph and reading off the concentration at which 50% of cells remain viable relative to the control. Each experiment was repeated at least three times to get the mean values. Four different tumor cell lines were the subjects of this study: MCF-7, Hela, BEL-7402, and MG-63 (purchased from American Type Culture Collection).

2.6. *Apoptosis studies*

Apoptosis studies were performed with a staining method utilizing acridine orange (AO) and EB [25]. According to the difference in membrane integrity between necrotic and apoptosis, AO can pass through cell membrane, but EB cannot. Under fluorescence microscope, live cells appear green. Necrotic cells stain red but have a nuclear morphology resembling that of viable cells. Apoptosis cells appear green, and morphological changes such as cell blebbing and formation of apoptotic bodies are observed.

A monolayer of BEL-7402 cells was incubated in the absence and presence of **1** at 25 μmol L^{-1} at 37°C and 5% CO_2 for 24 h. After 24 h, the cells were stained with AO/EB solution (100 μgmL^{-1} AO, 100 μgmL^{-1} EB). Then the samples were observed under a fluorescence microscope.

2.7. *Antioxidant activity*

The hydroxyl radical (•OH) in aqueous medium was generated by the Fenton system [26]. The solution of the tested complexes was prepared with DMF. The assay mixture (5 mL) contained safranin (28.5 μmol L^{-1}), EDTA-Fe(II) (100 μmol L^{-1}), H_2O_2 (44.0 μmol L^{-1}), the tested compounds (2.5–17.5 μmol L^{-1}), and a phosphate buffer (67 mmol L^{-1}, pH = 7.4). The assay mixtures were incubated at 37°C for 30 min in a water bath and then the absorbance was measured at 520 nm. All tests were run in triplicate and expressed as the mean. A_i was the absorbance in the presence of the tested compound; A_0 was the absorbance in the absence of tested compounds; A_c was the absorbance in the absence of tested compound, EDTA-Fe(II), and H_2O_2. The suppression ratio (η_a) was calculated on the basis of $(A_i - A_0)/(A_c - A_0) \times 100\%$.

3. Results and discussion

3.1. *Electronic absorption titration*

In order to assess the DNA-binding behaviors of **1** and **2**, absorption titrations were carried out. As shown in figure 1, as the CT-DNA concentration is increased, the

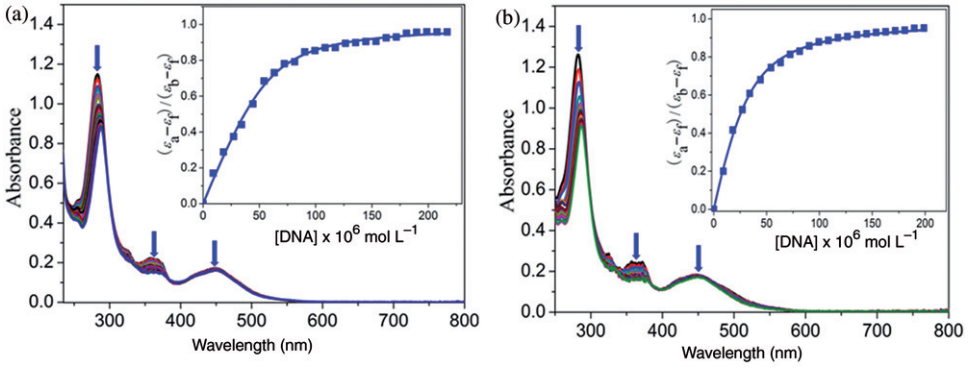

Figure 1. Absorption spectra in Tris-HCl buffer upon addition of CT-DNA in the presence of (a) **1** and (b) **2**. [Ru] = 10 μmol L^{-1}. Arrow shows the absorbance change upon increasing DNA concentration. Plots of $(\varepsilon_a - \varepsilon_f)/(\varepsilon_b - \varepsilon_f)$ *vs.* [DNA] for titration of DNA with Ru(II) complexes.

MLCT bands of **1** at 448 nm and **2** at 447 nm exhibit hypochromism of 12.08% and 9.37% and bathochromism of 1 nm and 2 nm, respectively. However, much more pronounced hypochromism of 29.82% for **1** at 283 nm and 18.63% for **2** at 282 nm were observed. Although these results are different from observations on the interaction of DNA with some mononuclear Ru(II) complexes [27, 28], which gave simultaneous decreases in absorption for both UV and visible (MLCT) bands, considering the spectral overlap with the MLCT transitions, these spectral characteristics obviously suggest that **1** and **2** interact with DNA most likely through intercalation of bridging planar aromatic ring into the base pairs of DNA. Hiort *et al.* [29] deduced that for the $[Ru(phen)_2dppz]^{2+}$-DNA system, dppz intercalates into the DNA base pairs because the hypochromism of the intraligand transition of dppz is greater than that of MLCT. The values of K for **1** and **2** are 6.6 $(\pm 0.7) \times 10^5$ $(mol\,L^{-1})^{-1}$ ($s = 2.83$) and 1.6 $(\pm 0.2) \times 10^5$ $(mol\,L^{-1})^{-1}$ ($s = 1.44$), respectively. The values are larger than those of $[Ru(dmp)_2(APIP)]^{2+}$ (APIP = 2-(2-aminophenyl)imidazo[4,5-f][1,10]phenanthroline, 2.3×10^4 $(mol\,L^{-1})^{-1}$) [30] and $[Ru(dmb)_2(BFIP)]^{2+}$ (BFIP = 2-benzo[b]furan-2-yl-1H-imidazo[4,5-f][1,10]phenanthroline, 3.2×10^4 $(mol\,L^{-1})^{-1}$) [31], and comparable to those of DNA intercalators $[Ru(tpy)(ptp)]^{2+}$ (tpy = 2,2′:6′,2″-terpyridine, ptp = 3-(1,10-phenanthrolin-2-yl)-*as*-triazino[5,6-*f*]phenanthrene, 1.62×10^5 $(mol\,L^{-1})^{-1}$) [32], $[Ru(bpy)_2(taptp)]^{2+}$ (taptp = 4,5,9,18-tetraazaphenanthreno[9,10-*b*]triphenylene, 1.7×10^5 $(mol\,L^{-1})^{-1}$) [33], $[Ru(MeIm)_4(tip)]^{2+}$ (MeIm = 1-methylimidazole, tip = 2-(thiophene-2group)-1H-imidazo[4,5-f][1,10]phenanthroline, 7.20×10^5 $(mol\,L^{-1})^{-1}$) [34], but is not as strong as that of their parent complexes $[Ru(bpy)_2(dppz)]^{2+}$ (4.9×10^6 $(mol\,L^{-1})^{-1}$) [35] and $[Ru(dmb)_2(dppz)]^{2+}$ (4.5×10^6 $(mol\,L^{-1})^{-1}$) [36].

3.2. *Luminescence studies and continuous variation analysis*

Emission intensities of **1** and **2** from their MLCT excited states upon excitation at 448 and 447 nm are found to depend on DNA concentration. For each titration of CT-DNA, luminescence enhancements occur within minutes of DNA addition, indicating that association rates are relatively rapid. As shown in figure 2, as the

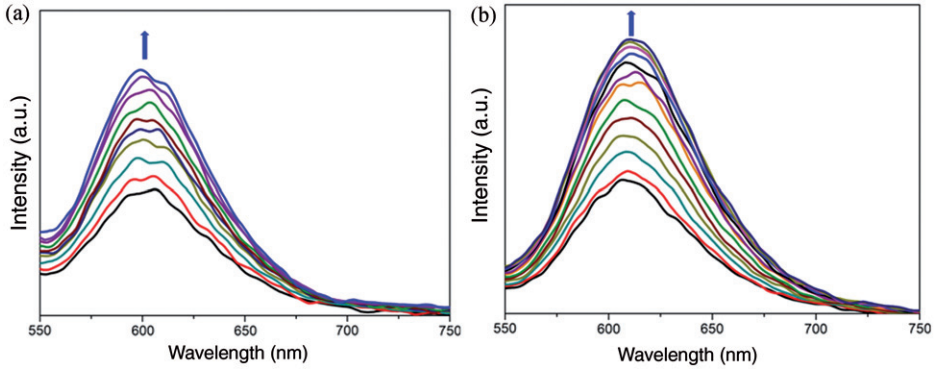

Figure 2. Emission spectra of (a) **1** and (b) **2** in Tris-HCl buffer in the absence and presence of CT-DNA. Arrow shows the intensity change upon increasing DNA concentration.

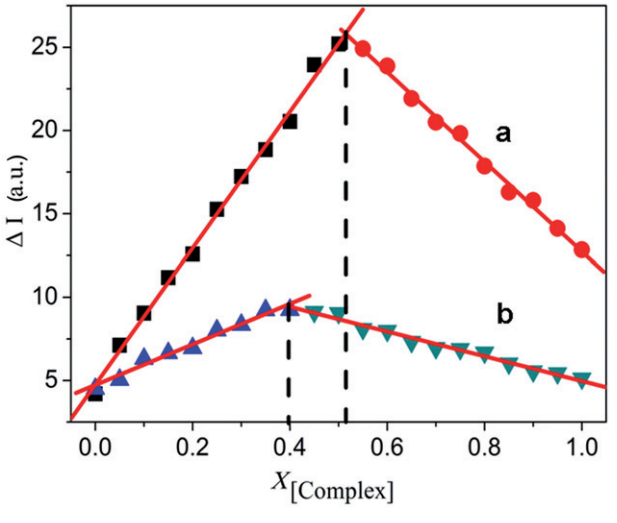

Figure 3. Job plot using luminescence data for complexes **1** (a) and **2** (b) with CT DNA in Tris-HCl buffer, pH = 7.0.

concentration of CT-DNA increased, the emission intensities of **1** (at 602 nm) and **2** (at 610 nm) were about 1.82 and 2.06 times larger than the original. The enhancement of emission intensity is an indication of binding of the complex to the hydrophobic pocket of DNA, and the complex can be protected efficiently by the hydrophobic environment inside the DNA helix.

Binding stoichiometry with CT-DNA was then investigated through the luminescence-based Job plot (figure 3). One major inflection point for **1** and **2** was observed at $\chi = 0.52$ and 0.40, respectively. These data were consistent with a 1 : 1 and 1.5 : 1 [DNA]/[complex] binding mode. Compared with that obtained from electronic titration, the binding size obtained from continuous variation analysis is different from that obtained

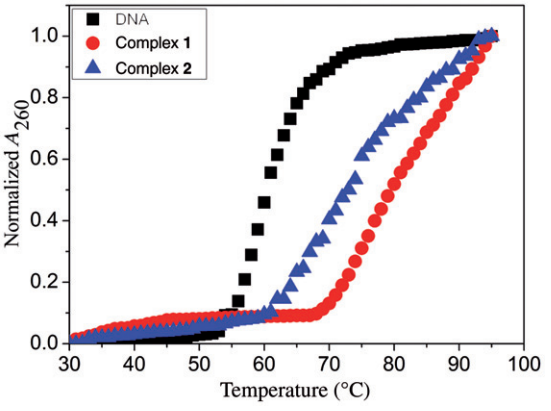

Figure 4. Thermal denaturation of CT-DNA in the absence (■) and presence of complexes 1 (●) and 2 (▲). [Ru] = 10 μM, [DNA] = 100 μM.

from electronic titration. This difference between the two sets of binding sizes could be caused by the different spectroscopy and calculation method.

3.3. *DNA thermal denaturation studies*

Thermal behavior of DNA in the presence of complexes can give insight into their conformational changes when temperature is raised, and offer information about the interaction strength of complexes with DNA. When the temperature in the solution increases, the double-stranded DNA gradually dissociates to single strands [37] and generates a hyperchromic effect on the absorption spectra of DNA bases ($\lambda_{max} = 260$ nm). In order to identify this transition process, the melting temperature T_m, which is defined as the temperature where half of the total base pairs is unbonded, is usually introduced. According to previous literatures [35, 36], the intercalation of natural or synthesized organics and metallointercalators generally results in a considerable increase in melting temperature (T_m). The melting curves of CT-DNA in the absence and presence of the complex are presented in figure 4. The thermal denaturation experiment carried out for DNA in the absence of the Ru(II) complexes revealed a T_m of 60.7 ± 0.1°C under our experimental conditions. The observed melting temperature in the presence of **1** and **2** was 79.2 ± 0.2°C and 72.3 ± 0.2°C, respectively, at a concentration ratio [Ru]/[DNA] = 1 : 10. The large increases in T_m of two Ru(II) complexes (the ΔT_m is 18.5°C and 11.6°C for **1** and **2**, respectively) are comparable to that observed for classical intercalators [38, 39].

3.4. *Viscosity measurements*

To investigate further the DNA-binding mode of **1** and **2**, viscosity measurements on solutions of CT-DNA incubated with the complexes were performed. Partial and/or nonclassical intercalation of ligand could bend (or kink) the DNA helix, reducing its effective length and, concomitantly, its viscosity; a classical intercalation of ligand into DNA causes a significant increase in the viscosity of DNA solution due to an increase in

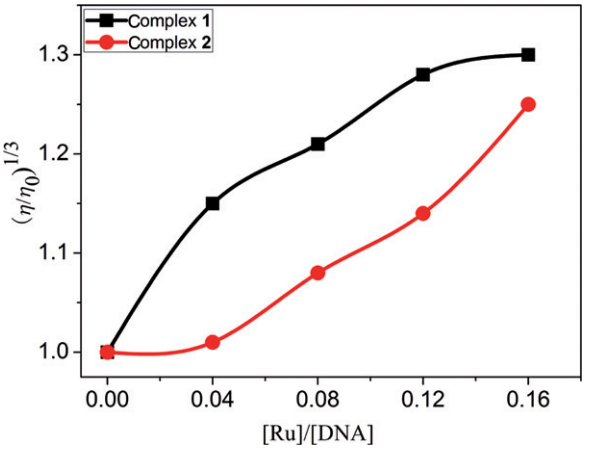

Figure 5. Effect of increasing amounts of **1** (■) and **2** (•) on the relative viscosity of CT-DNA at 25 (±0.1)°C. [DNA] = 0.30 mmol L^{-1}.

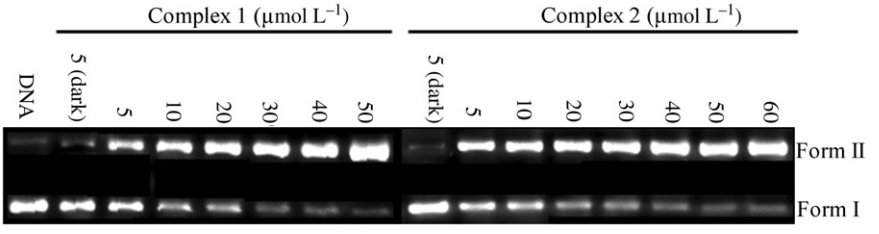

Figure 6. Photoactivated cleavage of pBR 322 DNA in the absence and presence of different concentrations of **1** and **2** after irradiation at 365 nm for 30 min.

the separation of the base pairs at the intercalation site and, hence, an increase in the overall DNA molecular length [40]. When **1** and **2** are treated with CT-DNA (0.30 mmol L^{-1}) and the concentrations of ruthenium complexes are increased from a ratio of $R = 0$–0.16 ($R = [Ru]/[DNA]$), the relative viscosity of DNA increases steadily (figure 5) in the order **1** > **2**. These results showed that **1** and **2** interact with DNA through intercalation. The large increase in the relative viscosity revealed that **1** is a better intercalator than **2**, which is consistent with our foregoing hypothesis.

3.5. *Photoactivated cleavage of pBR322 DNA*

When circular plasmid DNA is subject to electrophoresis, relatively fast migration will be observed for the intact supercoil form (Form I). If scission occurs on one strand (nicking), the supercoil relaxes to generate a slower moving open circular form (Form II). If both strands are cleaved, a linear form (Form III) is generated, which migrates between Forms I and II DNA [41]. The cleavage reactions on plasmid DNA induced by ruthenium(II) complexes were performed and monitored by agarose gel electrophoresis. Figure 6 shows gel electrophoresis separation of pBR322 DNA after incubation with

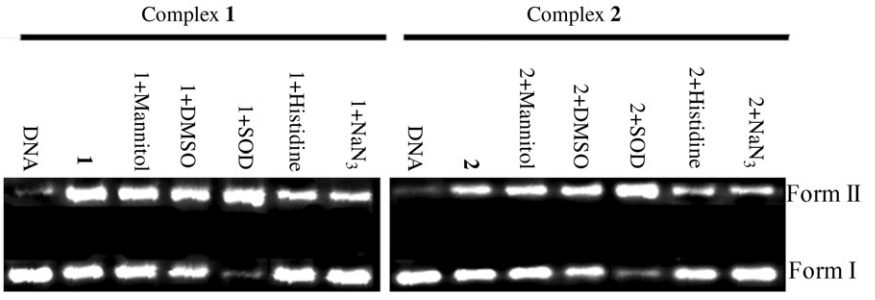

Figure 7. Photocleavage of supercoiled pBR322 DNA by **1** and **2** (10 μmol L^{-1}) in the absence and presence of different inhibitors [100 mmol L^{-1} mannitol, 200 mmol L^{-1} DMSO, 1000 Um L^{-1} SOD, 1.2 mmol L^{-1} histidine, 10 mmol L^{-1} NaN_3] after irradiation at 365 nm for 30 min.

different concentrations of Ru(II) complexes and irradiation at 365 nm for 30 min. No obvious DNA cleavage was observed for control in which complex was absent, or incubation of the plasmid with the Ru(II) complex in the dark. Upon increasing concentrations of **1** and **2**, the amount of Form I (supercoiled form) of pBR 322 DNA diminishes gradually, whereas that of Form II (circular form) increases. These results indicate that scission occurs on one strand (nicked). Under the same experimental conditions, **1** exhibits more effective DNA cleavage than **2**. The different cleaving efficiency is consistent with DNA-binding affinity of two Ru(II) complexes.

In order to establish the reactive species responsible for photoactivated cleavage of the plasmid, the influence of different potentially inhibiting agents was investigated. Figure 7 shows that DNA cleavage of the plasmid by **1** and **2** was not inhibited in the presence of hydroxyl radical (•OH) scavengers such as mannitol [42] and DMSO [43], which indicated that hydroxyl radical was not likely to be the cleaving agent. In the presence of superoxide dismutase (SOD), a facile superoxide anion radical ($O_2^{\bullet -}$) quencher, the cleavage was improved. The DNA cleavage of the plasmid was inhibited in the presence of singlet oxygen ($^1O_2$) scavenger histidine and NaN_3 [44, 45], suggesting that $^1O_2$ is likely to be the reactive species responsible for cleavage. Enhancement by SOD and inhibition by singlet oxygen scavengers have been observed by other ruthenium intercalators [46–48].

3.6. *Cytotoxicity assay* in vitro

The cytotoxicity *in vitro* assay for complexes was assessed using the method of MTT reduction. Cisplatin was used as a positive control. After treatment of MCF-7, Hela, BEL-7402, and MG-63 cell lines for 72 h with **1** and **2** in the range of concentration (3.13 → 200 μmol L^{-1}), the inhibitory percentage against growth of cancer cells was determined. The cell viabilities (%) obtained with continuous exposure for 72 h are depicted in figure 8. The cytotoxicity was concentration-dependent. Cell viability decreased with increasing concentrations of **1** and **2**. The IC_{50} values were calculated and are listed in table 1. The IC_{50} values are 16.4, 21.2, 32.6, and 34.8 for **1**, 20.5, 37.2, 16.8, and 33.2 for **2** toward MCF-7, Hela, BEL-7402, and MG-63 cells, respectively. Comparing **1** and **2**, **1** is more cytotoxic against the cell lines of MCF-7 and Hela. Furthermore, all these complexes showed relatively lower cytotoxicity than cisplatin.

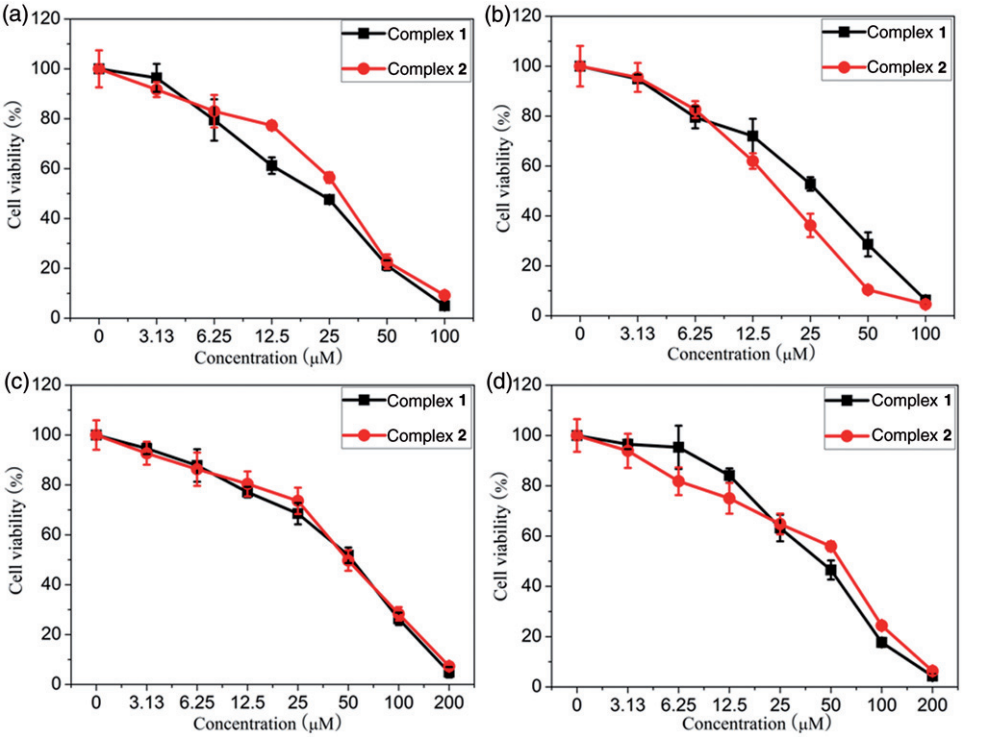

Figure 8. Cell viability of **1** and **2** on tumor MCF-7 (a), Hela (b), BEL-7402 (c), and MG-63 (d) cell proliferation *in vitro*. Each data point is the mean ± standard error obtained from at least three independent experiments.

Table 1. The IC_{50} values for **1** and **2** against selected cell lines.

	IC_{50} ($\mu mol\,L^{-1}$)			
Complex	MCF-7	Hela	BEL-7402	MG-63
1	16.4	21.2	32.6	34.8
2	20.5	37.2	16.8	33.2
Cisplatin	12.2	10.5	13.4	–

3.7. *Apoptosis studies*

Cell death was divided into two types, necrosis (accidental cell death) and apoptosis (programmed cell death) [49]. Necrosis causes inflammation while apoptosis does not. Induction of tumor cell apoptosis has been used as an important indicator to detect the ability of chemotherapeutic drugs to inhibit tumor growth [50]. The type of cell death induced by **1** and **2** was investigated by the apoptosis assay AO/EB staining. The AO/EB staining assay can detect the difference in membrane integrity between necrotic and apoptotic cells [25]. AO is a vital dye and can stain both live and dead cells. EB stains

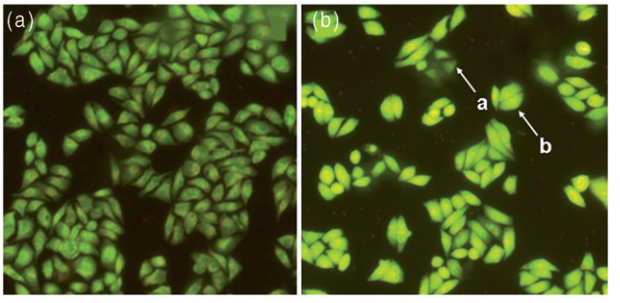

Figure 9. BEL-7402 cells were stained by AO/EB and observed under fluorescence microscopy. BEL-7402 cells without treatment (a) and in the presence of **1** (b, 25 μmol L^{-1}) incubated at 37°C and 5% CO_2 for 24 h; cells in a and b are living and apoptotic cells, respectively.

only cells that have lost their membrane integrity. Under the fluorescence microscope, live cells appear green. Necrotic cells stain red, but have a nuclear morphology resembling viable cells. Apoptotic cells appear green and morphological changes such as cell blebbing and formation of apoptotic bodies are observed. In the absence of **1**, living BEL-7402 cells were stained bright green in spots (figure 9a). However, after treatment with **1**, green apoptotic cells containing apoptotic bodies were also observed (figure 9b). Similar results were also observed for **2**. The results suggest that **1** and **2** can effectively induce the apoptosis of BEL-7402 cells.

3.8. *Antioxidant activity*

Oxidative damage to DNA has been suggested to contribute to aging and various diseases including cancer and chronic inflammation [51]. Among all reactive oxygen species, the hydroxyl radical (•OH) is by far the most potent and therefore the most dangerous oxygen metabolite, elimination of this radical is a major aim of antioxidant administration [52]. The hydroxyl radical (•OH) in aqueous media is generated by the Fenton system. The antioxidant activity of **1** and **2** was investigated. The inhibitory effect is depicted in figure 10 and the suppression ratio is listed in table 2. The average suppression ratio valued from 1.83% to 75.92% for **1**, 0.86% to 85% for **2**. The antioxidant activity against hydroxyl radical of **1** and **2** is comparable under the same experimental conditions. It is clear that **1** and **2** have high antioxidant activity. Similar results were observed for other ruthenium(II) complexes [53]. The information obtained from this work could help in developing new antioxidants and therapeutic reagents for some diseases.

4. Conclusion

Two new ruthenium(II) polypyridine complexes, $[Ru(bpy)_2(DMDPPZ)](ClO_4)_2$ (**1**) and $[Ru(dmb)_2(DMDPPZ)](ClO_4)_2$ (**2**), have been synthesized and characterized. The DNA-binding of these complexes with CT-DNA indicate that the two complexes intercalate between DNA base pairs. Both complexes cleave plasmid DNA when

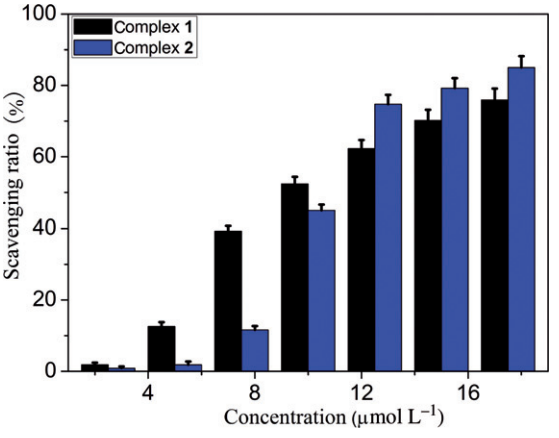

Figure 10. Scavenging effect of **1** and **2** on hydroxyl radicals. Experiments were performed in triplicate.

Table 2. The scavenging ratios (%) of complexes against •OH.

	Average inhibition (%) for •OH (μmol L^{-1})						
Complex	2.5	5	7.5	10	12.5	15	17.5
1	1.83	12.57	39.27	52.36	62.30	70.16	75.92
2	0.86	1.84	11.58	45.00	74.74	79.21	85.00

irradiated at 365 nm for 30 min. The studies of mechanism on photocleavage demonstrate that superoxide anion radical ($O_2^{\bullet -}$) and singlet oxygen ($^1O_2$) may play important roles. The data obtained from continuous variation analysis were consistent with a 1 : 1 and 1.5 : 1 [DNA]/[complex] binding mode for **1** and **2**, respectively. Cytotoxicity assay *in vitro* showed that **1** and **2** displayed moderate antitumor activities against selected tumor cell lines and can induce apoptosis of BEL-7402 cells. Antioxidant activity experiments showed good antioxidant activity against hydroxyl radical (•OH). The results should be of value in further understanding DNA-binding and antitumor activity by Ru(II) complexes, as well as laying the foundation for discovery of new antitumor agents.

Acknowledgments

This work was supported by the National Nature Science Foundation of China (Nos. 30800227 and 31070858) and Guangdong Pharmaceutical University.

References

[1] G. Marcon, S. Carotti, M. Coronnello, L. Messori, E. Mini, P. Orioli, T. Mazzei, M.A. Cinellu, G. Minghetti. *J. Med. Chem.*, **45**, 1672 (2002).

[2] P.J. Dyson, M.J. Rose, N.L. Fry, R. Marlow, L. Hinck, P.K. Mascharak. *J. Am. Chem. Soc.*, **130**, 8834 (2008).
[3] Z. Wu, Q. Liu, X. Liang, X. Yang, N. Wang, X. Wang, H. Sun, Y. Lu, Z. Guo. *JBIC, J. Biol. Inorg. Chem.*, **14**, 1313 (2009).
[4] M.H. Lim, H. Song, E.D. Olmon, E.E. Dervan, J.K. Barton. *Inorg. Chem.*, **48**, 5392 (2009).
[5] Y.J. Sun, L.E. Joyce, N.M. Dickson, C. Turro. *Chem. Commun.*, **46**, 2426 (2010).
[6] I. Bratsos, S. Jedner, T. Gianferrara, E. Alessio. *Chimia*, **61**, 692 (2007).
[7] X. Meng, M.L. Leyva, M. Jenny, I. Gross, S. Benosman, B. Harlepp, P. Hébraud, A. Boos, P. Wlosik, P. Bischoff, C. Sirlin, M. Pfeffer, J.P. Loeffler, C. Gaiddon. *Cancer Res.*, **69**, 5458 (2009).
[8] T.F. Chen, Y.N. Liu, W.J. Zhen, J. Liu, Y.S. Wong. *Inorg. Chem.*, **49**, 6366 (2010).
[9] U. Schatzschneider, J. Niesel, I. Ott, R. Gust, H. Alborzinia, S. Wölfl. *Chem-Med Chem*, **3**, 1104 (2008).
[10] Y.J. Liu, C.H. Zeng, H.L. Huang, L.X. He, F.H. Wu. *Eur. J. Med. Chem.*, **45**, 564 (2010).
[11] J.G. Liu, Q.L. Zhang, X.F. Shi, L.N. Ji. *Inorg. Chem.*, **40**, 5045 (2001).
[12] P.U. Maheswari, V. Rajendiran, M. Palaniandavar, R. Parthasarathi, V. Subramanian. *J. Inorg. Biochem.*, **100**, 3 (2006).
[13] T. Biver, C. Cavazza, F. Secco, M. Venturini. *J. Inorg. Biochem.*, **101**, 461 (2007).
[14] J. Marmur. *J. Mol. Biol.*, **3**, 208 (1961).
[15] M.E. Reichmann, S.A. Rice, C.A. Thomas, P. Doty. *J. Am. Chem. Soc.*, **76**, 3047 (1954).
[16] B.P. Sullivan, D.J. Salmon, T.J. Meyer. *Inorg. Chem.*, **17**, 3334 (1978).
[17] M. Yamada, Y. Tanaka, Y. Yoshimoto, S. Kuroda, I. Shimao. *Bull. Chem. Soc. Japan*, **65**, 1006 (1992).
[18] M.T. Carter, M. Rodriguez, A. Bard. *J. Am. Chem. Soc.*, **111**, 8901 (1989).
[19] J.B. Chaires, N. Dattagupta, D.M. Crothers. *Biochemistry*, **21**, 3933 (1982).
[20] S. Satyanarayana, J.C. Dabrowiak, J.B. Chaires. *Biochemistry*, **32**, 2573 (1993).
[21] S. Satyanarayana, J.C. Dabrowiak, J.B. Chaires. *Biochemistry*, **31**, 9319 (1992).
[22] G. Cohen, H. Eisenberg. *Biopolymers*, **8**, 45 (1969).
[23] P. Job. *Ann. Chim. (Paris)*, **9**, 113 (1928).
[24] T. Mosmann. *J. Immunol. Methods*, **65**, 55 (1983).
[25] G.P. Amarante-Mendes, E. Bossy-Wetzel, T. Brunner, D. Finucane, D.R. Green, S. Kasibhatla. In *Cells: A Laboratory Manual*, D.L. Spector, R.D. Goldman, L.A. Leinwand (Eds), Vol. 1, Chap. 15, pp. 3–6, Cold Spring Harbor Laboratory Press, New York (1998).
[26] J.A. Hickman. *Cancer Metast. Rev.*, **11**, 121 (1992).
[27] X.H. Zhou, B.H. Ye, H. Li, J.G. Liu, Y. Xiang, L.N. Ji. *J. Chem. Soc., Dalton Trans.*, 1423 (1999).
[28] R.B. Nair, E.S. Teng, A.L. Kirkland, C.J. Murphy. *Inorg. Chem.*, **37**, 139 (1998).
[29] C. Hiort, P. Lincoln, B. Nordén. *J. Am. Chem. Soc.*, **115**, 3448 (1993).
[30] Z.H. Liang, Z.Z. Li, H.L. Huang, Y.J. Liu. *J. Coord. Chem.*, **64**, 3342 (2011).
[31] K.A. Kumar, K.L. Reddy, S. Satyanarayana. *J. Coord. Chem.*, **63**, 3676 (2010).
[32] H. Chao, W.J. Mei, Q.W. Huang, L.N. Ji. *J. Inorg. Biochem.*, **92**, 165 (2002).
[33] Q.X. Zhen, B.H. Ye, Q.L. Zhang, J.G. Liu, H. Li, L.N. Ji, L. Wang. *J. Inorg. Biochem.*, **76**, 47 (1999).
[34] X.C. Yang, Y.N. Liu, S.T. Yao, Y. Xia, Q. Li, W.J. Zheng, L.M. Chen, J. Liu. *J. Coord. Chem.*, **64**, 1491 (2011).
[35] A.E. Friedman, J.C. Chambron, J.P. Sauvage, N.J. Turro, J.K. Barton. *J. Am. Chem. Soc.*, **112**, 4960 (1990).
[36] J.G. Liu, Q.L. Zhang, X.F. Shi, L.N. Ji. *Inorg. Chem.*, **40**, 5045 (2001).
[37] E. Tselepi-Kalouli, N. Katsaros. *J. Inorg. Biochem.*, **37**, 271 (1989).
[38] M.J. Waring. *J. Mol. Biol.*, **13**, 269 (1965).
[39] G.A. Neyhart, N. Grover, S.R. Smith, W.A. Kalsbeck, T.A. Fairly, M. Cory, H.H. Thorp. *J. Am. Chem. Soc.*, **115**, 4423 (1993).
[40] S. Satyanarayana, J.C. Dabrowiak, J.B. Chaires. *Biochemistry*, **32**, 2573 (1993).
[41] J.K. Barton, A.L. Raphael. *J. Am. Chem. Soc.*, **106**, 2466 (1984).
[42] C.C. Cheng, S.E. Rokita, C.J. Burrows. *Angew. Chem. Int. Ed. Engl.*, **32**, 277 (1993).
[43] S.A. Lesko, R.J. Lorentzen, P.O.P. Ts'o. *Biochemistry*, **19**, 3023 (1980).
[44] R. Nilsson, P.B. Merkel, D.R. Kearns. *Photochem. Photobiol.*, **16**, 117 (1972).
[45] A.K. Patra, M. Nethaji, A.R. Chakravarty. *J. Inorg. Biochem.*, **101**, 233 (2007).
[46] F. Gao, H. Chao, F. Zhou, Y.X. Yuan, B. Peng, L.N. Ji. *J. Inorg. Biochem.*, **100**, 1487 (2006).
[47] H.J. Yu, S.M. Huang, L.Y. Li, H.N. Ji, H. Chao, Z.W. Mao, J.Z. Liu, L.N. Ji. *J. Inorg. Biochem.*, **103**, 881 (2009).
[48] Y.J. Liu, C.H. Zeng, F.H. Wu, J.H. Yao, L.X. He, H.L. Huang. *J. Mol. Struct.*, **932**, 105 (2009).
[49] I. Vermes, C. Haanen. *Adv. Clin. Chem.*, **31**, 177 (1994).
[50] T. Zhang, X. Chen, L. Qu, J. Wu, R. Cui, Y. Zhao. *Bioorg. Med. Chem.*, **12**, 6097 (2004).
[51] K. Tsai, T.G. Hsu, K.M. Hsu, H. Cheng, T.Y. Liu, C.F. Hsu, C.W. Kong. *Free Radical Biol. Med.*, **31**, 1465 (2001).
[52] N. Udilova, A.V. Kozlov, W. Bieberschulte, K. Frei, K. Ehrenberger, H. Nohl. *Biochem. Pharm.*, **65**, 59 (2003).
[53] H.L. Huang, Y.J. Liu, C.H. Zeng, L.X. He, F.H. Wu. *DNA Cell Biol.*, **29**, 261 (2010).